Rotational motions of seismic surface waves in a laterally heterogeneous Earth

Manuscript submitted to the BSSA special issue on Rotational Seismology and Engineering Applications

September 24, 2008

Ana MG Ferreira (1, 2) and Heiner Igel (3)

(1) School of Environmental Sciences, University of East Anglia, Norwich NR4 7TK, UK

(2) ICIST, IST, Technical University of Lisbon, 1049-001 Lisbon, Portugal

(3) Department of Earth and Environmental Sciences, Ludwig-Maximilians-University Munich, Theresienstraße 41, D-80333 Munich, Germany

Abstract

A number of recent studies have analysed seismic rotational data using a relationship between transverse acceleration and rotation rate derived for a homogeneous full space. In this study we explore this relationship further theoretically by presenting a full ray theory (FRT) method to simulate rotational motions of **fundamental mode** seismic surface waves in smooth, laterally heterogeneous Earth models. In the ray picture of wave propagation the vertical component of the rotational rate motion of fundamental mode Love waves is obtained by dividing the transverse component of ground acceleration by the Love wave local phase velocity beneath the seismic recording station. We illustrate the method with examples of theoretical calculations of $T \approx 40s$ rotational rate ground motions of fundamental Love waves using the crust model CRUST2.0 combined with the mantle model S20RTS for the M8.1 September 25 2003 Tokachi-oki earthquake, Japan. FRT rotation synthetics match complete calculations using the spectral-element method very well and fit real data reasonably well. Furthermore, we show that the effect of realistic local structures beneath receivers on rotational motions is strong enough to be observable. FRT calculations could potentially help inferring Love wave local dispersion curves and thus estimating the 1-D local shear velocity structure beneath seismic stations from point measurements of rotational rate and acceleration ground motions.

1 Introduction

With the ever-increasing amount of seismic broadband data assembled from high-quality global networks (IRIS, GEOSCOPE, MedNet, Geofone and other national networks) three-dimensional global images of the Earth's mantle have greatly progressed over the last 30 years. However, standard seismic observations are restricted to three components of translations, despite the fact that in theory the recovery of the complete ground motion requires the observation of three additional components of rotations and six components of strain (e.g. Aki & Richards, 2002; Trifunac & Todorovska, 2001).

In the past years, rotation sensor technology has been improving in a way that may lead to the development of routine sensors for three additional rotational motion components useful for seismological applications . **Using ring laser technology, rotation rates as small as** $10^{-10} rads^{-1}/\sqrt{Hz}$ **can be observed (e.g. Schreiber et al., 2006). These recent observations of rotational motions** showed that the rotational measurements are consistent with collocated observations of translations within the framework of linear elasticity (e.g. Igel et al., 2005, 2007; Cochard et al., 2006), following the earlier pioneering observations of earthquake-induced rotational motions by McLeod et al. (1998) and by Pancha et al. (2000).

Assuming plane wave propagation in a homogeneous and isotropic full space, one can show that at a given station the transverse acceleration and rotation rate (around a vertical axis) are in phase and their ratio is proportional to the horizontal phase velocity (e.g. Pancha et al., 2000; Igel et al., 2005). A similar relationship between strain and displacements can be used to determine horizontal phase velocities (e.g. Mikumo & Aki, 1964; Gomberg & Agnew, 1996). Igel et al. (2005, 2007) and Cochard et al. (2006) exploited this relationship to estimate horizontal phase velocities in sliding time windows

along the observed time series. Comparison with synthetic traces (rotations and translations) and phase velocities determined in the same way showed good agreement with the observations. These initial results suggested that the determination of Love-wave dispersion curves (and thus information on local 1-D shear velocity structure) may be possible. This is remarkable in the sense that the estimation of the local dispersion curve would thus be based upon a point measurement rather than the observation of the wavefield across an array of seismometers. These experimental results are further supported by the recent application of the adjoint method to the combined measurement of rotations and translations (Fichtner & Igel, 2008). This study has shown that the sensitivity of such measurement to structural properties is concentrated around the receiver location, indicating the possibility of developing a novel kind of seismic tomography based upon joint measurements of translations and rotations. In the light of this, it is worth exploring further theoretically the relationship between rotations and translations and their use to estimate Love-wave dispersion curves.

In this study we simulate fundamental Love wave rotation and translation motions in global Earth models (both spherically symmetric and three-dimensional). We start by describing rotational motions of seismic waves in a spherically symmetric Earth model using a mode summation formalism. We then extend this approach to smooth, laterally varying Earth models using surface wave full ray theory (FRT) (Woodhouse, 1974; Woodhouse & Wong, 1986; Tromp & Dahlen, 1992a,b; Ferreira & Woodhouse, 2007). We compare FRT calculations with spectral-element method (SEM) simulations (Komatitsch & Tromp, 2002a,b) and with real data. Furthermore, we use FRT to illustrate the influence of various local structures on Love wave rotational motions and we discuss the potential use of FRT in real data applications.

2 Modelling

2.1 Free oscillations in spherically symmetric Earth models

In a spherically symmetric, nonrotating, perfectly elastic, isotropic (SNREI) Earth model, and for a point source, the ground velocity following an earthquake can be obtained by calculating the excitation of each mode of vibration and then summing the ground velocity associated with each mode at the receiver (eg Gilbert, 1970; Gilbert & Dziewonski, 1975). For a given mode of vibration ω_l^m having unit excitation we can write the ground velocity spectrum as:

$$\dot{\mathbf{s}}(\mathbf{r},\omega) = \omega U \hat{\mathbf{r}} Y_l^m + \omega V \frac{\nabla_1 Y_l^m}{\sqrt{l(l+1)}} - \omega W \frac{\hat{\mathbf{r}} \times \nabla_1 Y_l^m}{\sqrt{l(l+1)}}, \tag{2.1}$$

where U, V, W are the **vertical, longitudinal and transverse** scalar modal eigenfunctions evaluated at the Earth's surface, $Y_l^m = Y_l^m(\theta,\phi)$ are the real scalar spherical harmonics and ∇_1 represents the tangential gradient operator on the unit sphere, $\nabla_1 = \hat{\theta}\partial_\theta + \hat{\mathbf{\Phi}} cosec\theta \partial_\phi$ **(for more details see e.g. Gilbert & Dziewonski (1975))**. It follows that the curl of the ground velocity - the rotational rate motion - is given by (see e.g. Dahlen & Tromp, 1998):

$$\frac{1}{2}\nabla \times \dot{\mathbf{s}} = \omega \frac{\sqrt{l(l+1)}}{2a} W\, \hat{\mathbf{r}} Y_l^m + \frac{\omega}{2}\left(\frac{dW}{dr} + \frac{W}{a}\right)\frac{\nabla_1 Y_l^m}{\sqrt{l(l+1)}} + \frac{\omega}{2}\left(\frac{dV}{dr} + \frac{1}{a}\left(V - \sqrt{l(l+1)}U\right)\right)\frac{\hat{\mathbf{r}} \times \nabla_1 Y_l^m}{\sqrt{l(l+1)}}, \tag{2.2}$$

where a is the radius of the Earth. Equations 2.1–2.2 describe the velocity and rotational rate motion response as a superposition of standing waves or normal modes. Alternatively, it is possible to decompose the response into a sum of traveling waves,

which corresponds to the asymptotic limit of large angular order l . For large angular orders $l >> 1$, the vertical component of the rotation rate vector $\dot{\Omega}_r$ for a given mode of vibration ω_l^m becomes:

$$\hat{\mathbf{r}} \cdot \frac{1}{2}\nabla \times \dot{\mathbf{s}} = \dot{\Omega}_r = \omega \frac{(l+1/2)}{2a} W Y_l^m = \omega \frac{k}{2} W Y_l^m \tag{2.3}$$

where we have used the fact that the asymptotic wavenumber k of a high-degree scalar spherical harmonic is $k = \frac{l+1/2}{a} = \frac{\lambda}{a}$ (see e.g. Dahlen & Tromp, 1998). On the other hand, the transverse component of ground acceleration, $\ddot{s}_T$, for a given mode of vibration ω_l^m is given by (see Equation 2.1):

$$\ddot{s}_T = \omega^2 W Y_l^m \tag{2.4}$$

Thus, dividing Equation 2.3 by Equation 2.4 it follows that the ratio of vertical rotational motion to transverse ground velocity is given by:

$$\frac{\dot{\Omega}_r(\omega)}{\ddot{s}_T(\omega)} = \frac{k}{2\omega} = \frac{1}{2c_T(\omega)} \tag{2.5}$$

where c_T is the wave's horizontal phase velocity in the transverse direction. This shows that for a SNREI Earth model, at any frequency, the ratio between vertical rotational rate motion and transverse ground acceleration is given by half of the inverse of the transverse wave phase velocity.

2.2 Surface waves in smooth, laterally heterogeneous Earth models

Let us now focus on seismic surface waves, which correspond to an asymptotic limit of the complete sum over the normal-mode spectrum in Equation 2.1. From such limit (e.g. Dahlen & Tromp, 1998) and using Equation 2.5 it follows that the vertical component of the rotation rate motion vector of Love waves in a SNREI Earth model in the frequency domain is given by:

$$\dot{\Omega}_r(\mathbf{x}_s, \mathbf{x}_r; \omega) = \frac{\omega^2}{2c\, C}\, \mathbf{M} : E_s^*\, e^{i\frac{\pi}{4}} \sqrt{\frac{\lambda}{8\pi |\sin \Delta|}}\, e^{-i\lambda\Delta - \frac{\alpha_l \Delta}{C_l}}\, W, \tag{2.6}$$

for a source at position $\mathbf{x}_s$ and a receiver at $\mathbf{x}_r$. C is the Love wave angular group velocity, c is the Love wave phase velocity, $\mathbf{M}$ is the seismic moment tensor in spherical coordinates and $\mathbf{E}_s$ is the Love-wave strain tensor at the source, which involves the eigenfunction W and its radial derivative evaluated at the source's location. Δ is the angular epicentral distance and α_l is a decay factor related with the decay rate per cycle of the equivalent free oscillations, Q, $\alpha_l = \frac{\omega}{2Q}$.

For a smooth, laterally heterogeneous, transversely isotropic medium, we can write the full ray theory (or JWKB) rotation rate motion in a form analogous to Equation 2.6 (e.g. Tromp & Dahlen, 1992b; Ferreira & Woodhouse, 2007). The vertical component of the rotational rate motion response to a moment tensor $\mathbf{M}$ at hypocentral location $\mathbf{x}_s$ then becomes:

$$\dot{\Omega}_r(\mathbf{x}_s, \mathbf{x}_r; \omega) = \frac{\omega^2}{2} \underbrace{\frac{1}{\sqrt{C_s}}\, \mathbf{M} : E_s^*\, e^{i\frac{\pi}{4}}}_{source} \underbrace{\sqrt{\frac{\lambda}{8\pi S}}\, e^{\int_{path} (-i\lambda_l - \frac{\alpha_l}{C_l}) dl}}_{path} \underbrace{\frac{W_r}{c_r \sqrt{C_r}}}_{receiver}. \tag{2.7}$$

Equation 2.7 involves a source, a path and a receiver term and it differs from the expression for ground acceleration by a factor of $\frac{1}{2}c_r$, where c_r is the Love wave phase velocity at the receiver. We use a subscript s to denote evaluation at the source and a subscript r to denote evaluation at the receiver.

The Love wave strain tensor evaluated at the source, $\mathbf{E}_s$, now involves the local eigenfunction W_s and its radial derivative evaluated at the source's location (for explicit expressions see e.g. Ferreira & Woodhouse, 2007). **In practice we use the 1-D depth profile structure at the source's epicentral location, from the surface of the Earth down to its centre as predicted by existing 3-D tomographic models. The local eigenfunctions are calculated using a standard normal mode algorithm (Woodhouse, 1988) and it has been shown that the effect of local structures at the source on surface wave amplitudes is significant (Ferreira & Woodhouse, 2007).**

The path amplitude factor, $\sqrt{S}$, accounts for the geometrical spreading of monochromatic surface waves on a sphere, which reflects the focusing and defocusing of surface wave ray tubes due to heterogeneity. The path phase factor, $e^{\int_{path}(-i\lambda_l - \frac{\alpha_l}{C_l})dl}$, represents the phase delay due to propagation along the ray path, taking into account the anelastic attenuation of the waves. The path phase and amplitude are obtained by means of **exact** kinematic and dynamic ray tracing on the sphere **(see e.g. Woodhouse & Wong, 1986)**.

The receiver term depends on the local displacement eigenfunction at the receiver, W_r, and on the local phase and group velocities. **Like for the source term,** all the local eigenfunctions and local phase and group velocities are calculated, for a given local model, using a standard normal mode algorithm (for details on the numerical implementation see

Ferreira & Woodhouse, 2007). Calculations are carried out in the frequency domain at thirteen frequencies between 5 and 25 mHz, followed by spline interpolation in frequency. The time-domain Love-wave rotational motion synthetics are obtained through an inverse Fourier transformation.

Surface wave full ray theory assumes that there is no energy transfer from one mode branch to another, nor from Love to Rayleigh waves. While we expect that neglecting mode coupling is a good approximation for fundamental mode surface waves (see e.g. Tromp, 1994), for higher overtone branches mode coupling is more relevant. In this paper we focus on fundamental mode surface waves only, which are the prime data to image the upper mantle of the Earth, so we do not address the issue of mode coupling in detail.

A number of theoretical studies have addressed full ray theory to calculate seismic displacement seismograms ((Woodhouse, 1974; Woodhouse & Wong, 1986; Tromp & Dahlen, 1992b; Ferreira & Woodhouse, 2007)), but only two studies have actually implemented it numerically and showed examples of ground displacement synthetic seismogram calculations (Wang & Dahlen, 1994; Ferreira & Woodhouse, 2007). In the next sections we will show illustrative examples of the practical use of full ray theory to calculate rotational ground motions of fundamental Love waves for a smooth laterally varying Earth model.

3 Examples

3.1 Rotations at station WET, Wettzell

We here consider the vertical component of fundamental Love wave rotational rate motions at the station Wettzell, WET, at a latitude of 49.15^{o}N, longitude 12.88^{o}E, for the M8.1 September 25 2003 Tokachi-oki earthquake (Figure 1). The station WET is equipped with, among other instruments, a ring laser rotation sensor and a seismic broad-band sensor. We calculate rotations using earthquake source parameters from the Global CMT catalogue (Dziewonski et al., 1981) and we use the 3-D mantle model S20RTS (Ritsema et al., 1999) combined with the global crust model CRUST2.0 (Bassin et al., 2000). Within the crust, the local 1-D shear-wave velocity model beneath WET predicted by CRUST2.0 and S20RTS differs substantially from the global spherically symmetric model PREM (Dziewonski & Anderson, 1981) (Figure 2, a). Thus, the fundamental Love wave dispersion curve beneath WET obtained using the 1-D local model is different from the one obtained using PREM, particularly at higher frequencies, which are more sensitive to the crustal structure (Figure 2, b). Figure 3 compares rotational motions calculated using the spectral-element method (SEM) (Komatitsch & Tromp, 2002a,b) in the 3-D Earth model with calculations using FRT in the same model and with mode-summation calculations using PREM. All the traces are band-pass filtered around $T = 40s$. We see that there is poor agreement between the PREM synthetic and the SEM synthetic, with large phase and amplitude differences between the two traces. In contrast, FRT calculations match the SEM synthetic well. There are some discrepancies between the two traces in the early part of the wavetrains, probably because in this study full ray theory calculations do not include overtones (only fundamental modes are calculated).

We then compare FRT calculations with real data recorded by the ring-laser instrument at WET (Figure 4). There is reasonable agreement between the two waveforms, with some discrepancy in the amplitudes. Since the FRT calculations agree well with SEM predictions, these discrepancies must be due to uncertainties in the earthquake source model and/or to incorrect Earth structure rather than to theoretical limitations.

3.2 Influence of local structure beneath the receiver

Since full ray theory allows one to express waveforms in terms of a source, a path and a receiver term, it is an ideal tool to study the influence of local structures on observed waveforms. We here give examples of the effect of local structures beneath receivers on rotational ground motions by comparing two types of fundamental Love wave calculations:

(i) FRT synthetics in the 3-D Earth model;

(ii) "Receiver PREM" synthetics, which are calculated using full ray theory upon the 3-D Earth model applied only to the source and the path terms in Equation 2.7. The receiver term entering the full ray theory formulation (see Equation 2.7) is calculated using PREM.

Thus, for a given earthquake and recording station, discrepancies between these two types of theoretical calculations are due only to deviations of the local structure beneath the station from PREM.

We carry out calculations for the M8.1 September 25 2003 Tokachi-oki earthquake at a number of stations located in distinct tectonic environments with different crustal and mantle structures. Figure 5 shows comparisons of vertical component rotational rate motion FRT synthetics with "Receiver PREM" synthetics at four stations from the Global Seismic Network. Stations WET and LSA are located in distinct environments

within the interior of continents, with LSA being in the Tibetan plateau. Station GUMO is located in the Marianas ocean island and station LCO is located in the continental margin of Chile. For most stations we see that deviations in the local structure beneath the receiver from PREM lead to considerable differences in amplitude between the two types of rotational motion synthetics. This emphasizes the strong sensitivity of rotational motions to local structures at the receiver even for those predicted by smooth, long-wavelength Earth models such as CRUST2.0 combined with S20RTS. Comparing the differential synthetics for stations LSA and LCO with those in Figure 4, we see that the differences due to local structures at the receiver are comparable to differences between realistic 3-D calculations and real data. Hence, the effect of local structures at the receiver on Love wave rotational motion records must be strong enough to be observable, suggesting that rotational ground records can be used in practical applications to estimate the local structure beneath seismic receivers, particularly when combined with records of transverse ground acceleration at the same site.

4 Discussion

While applications to real data are beyond the scope of this paper, it is worthwhile to discuss some important practical aspects on how this work may be extended to real records of Love wave rotational rate and ground velocity (and particularly to their amplitude spectra analysis). Seismic surface wave amplitudes are rarely used in seismological applications because they are difficult to model and to measure. For example, sharp lateral variations in Earth structure along the source-receiver propagation path may lead to complications such as **ray focusing and defocusing**, ray bending, multipathing, coupling of Rayleigh waves with Love waves and interference with overtones and scattered waves. Thus, in order

to isolate the fundamental mode of Love waves in rotation rate and acceleration records, careful data selection and data analysis is needed to minimize these effects. For example, it is important to use earthquakes that are shallow to minimize overtone contamination **and mode coupling effects** and that are large enough to generate low-noise surface Love waves. Full ray theory is a valuable tool to select and analyze the data. In contrast to complete numerical wavefield calculations such as the spectral-element method, it allows us to simulate the propagation of fundamental mode Love waves alone using realistic 3-D Earth models. Thus, waveform comparisons between such calculations and real data allow us to assess the level of **overtone contamination and** interferences between the fundamental mode and other waves. Moreover, **ray focusing and defocusing and** ray bending effects are taken into account in FRT calculations and a multipathing detection is also included, enabling us to discard source-receiver pairs for which multipathing is predicted to occur (Ferreira, 2005; Ferreira & Woodhouse, 2007). Full ray theory calculations do not require substantial computational facilities and are computationally inexpensive, so it is feasible to use such calculations to select and analyze large data sets.

In contrast to global tomography, the problem of estimating local 1-D models involves a relatively small number of model parameters. Thus, Monte Carlo methods could be used to find the optimal local structures that minimize the misfit between theoretical and measured dispersion curves. Although only a standard normal mode algorithm would be needed for this purpose, FRT remains useful as it could be used to additionally assess the improvement in the fit between synthetics and recorded rotational waveforms during the model search. In contrast to numerical methods such as the spectral-element method, it is straightforward to implement different Earth models and notably to change local 1-D structures used in FRT calculations.

Full ray theory has limitations and a restricted domain of applicability, being valid in smooth media, when the wavelength of the propagating wave is smaller than the scale-length of heterogeneity in the Earth model along the propagation path. Thus, it remains to determine the exact domain of validity of the linear relationship between **fundamental mode surface wave** rotation rate and transverse acceleration. Future comparisons between full ray theory and spectral-element method calculations should allow us to establish exactly how small the wavelength must be compared with the scalelength of heterogeneity for the relationship to hold.

5 Conclusions

In this study we apply surface wave full ray theory to the problem of simulating Love waves (rotation and translations) for global Earth models (spherically symmetric and three-dimensional). We demonstrate that for smooth, laterally heterogeneous media the fundamental Love wave dispersion relation naturally appears as being proportional to the spectral ratio between transverse acceleration and rotation rate. The accuracy of full ray theory is confirmed by comparison with complete calculations using the spectral-element method. The sensitivity of rotational motions to local structure beneath the receiver is demonstrated with synthetic calculations for a global 3-D velocity model. This work suggests that FRT is a useful tool to help estimating local 1-D shear waves velocity structures beneath seismic stations.

6 Data and Resources

The records of the Tokachi-Oki event used in this study were provided by the Fundamentalstation Wettzell, and the Geophysics Section, Ludwig Maximilians University Munich and also previously discussed in Igel et al., 2005, 2007.

7 Acknowledgments

AMGF greatfully acknowledges support under a Royal Society grant 2007/R2. We are grateful to D. Komatitsch and J. Tromp for freely distributing their SEM code. HI gratefully acknowledges Dr. Lianjie Huang and the Los Alamos National Lab (EES-11) for a visiting fellowship in 2008.

References

Aki, K. & Richards, P., 2002. *Quantitative Seismology*, University Science Books; 2nd edition, San Francisco.

Bassin, C., Laske, G., & Masters, G., 2000. The current limits of resolution for surface wave tomography in North America, *EOS Trans. AGU*, **F897**, 81.

Cochard, A., Igel, H., Flaws, A., Schuberth, B., Wassermann, J., & Suryanto, W., 2006. Rotational motions in seismology: theory, observation, simulation, in *Earthquake source asymmetry, structural media and rotation effects*, edited by R. Teisseyre, M. Takeo, & E. Majewski, pp. 391–412, Springer Verlag.

Dahlen, F. A. & Tromp, J., 1998. *Theoretical Global Seismology*, Princeton University Press, New Jersey.

Dziewonski, A. M. & Anderson, D., 1981. Preliminary Reference Earth Model, *Phys. Earth Planet. Inter.*, **25**, 297–356.

Dziewonski, A. M., Chou, T.-A., & Woodhouse, J. H., 1981. Determination of earthquake source parameters from waveform data for studies of global and regional seismicity, *J. Geophys. Res.*, **86**(B4), 2825–2852.

Ferreira, A. M. G., 2005. *Seismic Surface Waves in the Laterally Heterogeneous Earth*, DPhil thesis, University of Oxford.

Ferreira, A. M. G. & Woodhouse, J., 2007. Source, path and receiver effects on seismic surface waves, *Geophys. J. Int.*, **168**, 109–232.

Fichtner, A. & Igel, H., 2008. Sensitivity densities for rotational ground motion measurements, *Bull. Seismol. Soc. Am.*, p. submitted.

Gilbert, F., 1970. Excitation of normal modes of the earth by earthquake sources, *Geophys. J. R. Astron. Soc.*, **22**, 223–226.

Gilbert, F. & Dziewonski, A. M., 1975. An application of normal mode theory to the retrieval of structural parameters and source mechanisms from seismic spectra, *Phil. Trans. R. Soc. Lond.*, **278**, 187–269.

Gomberg, J. & Agnew, D., 1996. The accuracy of seismic estimates of dynamic strains: An evalutation using strainmeter and seismometer data from pinon flat observatory, california, *Bull. Seismol. Soc. Am.*, **86**, 212–220.

Igel, H., Schreiber, U., Flaws, A., Schuberth, B., Velikoseltsev, A., & Cochard, A., 2005. Rotational motions induced by the M 8.1 Tokachi-oki earthquake, September 25, 2003, *Geophys. Res. Lett.*, **32**.

Igel, H., Cochard, A., Wassermann, J., Flaws, A., Schreiber, U., Velikoseltsev, A., & Pham, D. N., 2007. Broad-band observations of earthquake-induced rotational ground motions, *Geophys. J. Int.*.

Komatitsch, D. & Tromp, J., 2002. Spectral-element simulations of global seismic wave propagation—I. Validation, *Geophys. J. Int.*, **149**, 390–412.

Komatitsch, D. & Tromp, J., 2002. Spectral-element simulations of global seismic wave propagation—II. Three-dimensional models, oceans, rotation and self-gravitation, *Geophys. J. Int.*, **150**, 308–318.

McLeod, D., Stedman, G. E., Webb, T. H., & Schreiber, U., 1998. Comparison of standard and ring laser rotational seismograms, *Bull. Seismol. Soc. Am.*, **88**, 1495–1503.

Mikumo, T. & Aki, K., 1964. Determination of local phase velocity by intercomparison of seismograms from strain and pendulum instruments, *J. Geophys. Res.*, **69**, 721–731.

Pancha, A., Webb, T. H., Stedman, G., McLeod, P., & Schreiber, U., 2000. Ring laser detection of rotations from teleseismic waves, *Geophys. Res. Lett.*, **27**, 3553–3556.

Ritsema, J., van Heijst, H., & Woodhouse, J., 1999. Complex shear wave velocity structure imaged beneath Africa and Iceland, *Science*, **286**, 1925–1928.

Schreiber, U., Stedman, G., Igel, H., & Flaws, A., 2006. Ring laser gyroscopes as rotation sensors for seismic wave studies, in *Earthquake source asymmetry, structural media and rotation effects*, edited by R.Teisseyre, M. Takeo, & E. Majewski, pp. 377–390, Springer Verlag.

Trifunac, M. & Todorovska, M. I., 2001. A note on the useable dynamic range of accelerographs recording translation, *Soil Dyn. and Earth. Eng.*, **21**, 275–286.

Tromp, J., 1994. A coupled local-mode analysis of surface-wave propagation in a laterally heterogeneous waveguide, *Geophys. J. Int.*, **117**, 153–161.

Tromp, J. & Dahlen, F. A., 1992a. Variational principles for surface wave propagation on a laterally heterogeneous earth - I. Time-domain JWKB theory, *Geophys. J. Int.*, **109**, 581–598.

Tromp, J. & Dahlen, F. A., 1992b. Variational principles for surface wave propagation on a laterally heterogeneous earth - II. Frequency-domain JWKB theory, *Geophys. J. Int.*, **109**, 599–619.

Wang, Z. & Dahlen, F. A., 1994. JWKB surface-wave seismograms on a laterally heterogeneous earth, *Geophys. J. Int.*, **119**, 381–401.

Woodhouse, J. H., 1974. Surface waves in a laterally varying layered structure, *Geophys. J. R. Astron. Soc.*, **37**, 461–490.

Woodhouse, J. H., 1988. The calculation of the eigenfrequencies and eigenfunctions of the free oscillations of the earth and the sun, in *Seismological Algorithms*, edited by D. J. Doornbos, pp. 321–370.

Woodhouse, J. H. & Wong, Y. K., 1986. Amplitude, phase and path anomalies of mantle waves, *Geophys. J. R. Astron. Soc.*, **87**, 753–773.

8 Figure captions

Figure 1. Great-circle path (white line) between the epicenter of the M8.1 September 25 2003 Tokachi-oki earthquake, Japan (red star) and seismic station WET (Lat = 49.15^o, Lon = 12.88^o) near Wettzell, Germany (green triangle), at an epicentral distance of 80^o. These are superimposed on a T=40s fundamental Love wave phase velocity map calculated from the crust model CRUST2.0 combined with the mantle model S20RTS.

Figure 2. (a)Comparison between PREM shear-wave velocity model (solid line) and the local model beneath the seismic station WET predicted by the crustal model CRUST2.0 combined with the mantle model S20RTS (dashed line). (b) Theoretical local dispersion of fundamental Love waves as predicted by PREM (solid line) and by the local model beneath WET (dashed line).

Figure 3. (a) Comparison between spectral-element method (SEM) rotation rate synthetics around a vertical axis using the crustal model CRUST2.0 combined with the mantle model S20RTS (solid line) and mode-summation PREM rotation rate synthetics (dashed line) following the M8.1 September 25 2003 Tokachi-oki earthquake. (b) Comparison between SEM rotation synthetics using the crustal model CRUST2.0 and the mantle model S20RTS (solid line) and full ray theory (FRT) rotation rate synthetics using the same Earth model (dashed line). All the traces have been bandpass filtered around T=40s.

Figure 4. (a) Comparison between observed rotation rate motions around a vertical axis at station WET (solid line) and full ray theory rotation rate synthetics calculated using the crust model CRUST2.0 combined with the mantle model S20RTS (dashed line) for the M8.1 September 25 2003 Tokachi-oki earthquake. (b) Difference between the two

traces in the top diagram. All the traces have been bandpass filtered around T=40s.

Figure 5. Influence of local structure beneath the receiver for stations within different tectonic environments (green triangles): WET (Germany), LSA (Tibet), GUMO (Marianas Islands) and LCO (Chile). Seismograms are calculated for the M8.1 September 25 2003 Tokachi-oki earthquake (red star). The top diagrams (a,c,e,g) compare rotation rate full ray theory synthetics using the 3-D Earth model (solid line) with " Receiver PREM" synthetics, i.e., calculations using the 3-D Earth model to calculate the source and path terms in the full ray theory Equation 2.7 and using PREM to calculate the receiver term (dashed line); see section 3.2 for details. The traces in the bottom diagrams (b,d,f,h) show the differences between the two seismograms in the top. These differences are due only to deviations of the local shear-wave velocity structure beneath the receiver from PREM.

Figure 6. (a) Amplitude spectrum of the transverse component of an acceleration full ray theory synthetic calculated at station LCO for the M8.1 September 25 2003 Tokachi-oki earthquake, Japan. The synthetic has been calculated for fundamental Love waves using the crust model CRUST2.0 combined with the mantle model S20RTS. The amplitude spectrum has been estimated using the Thomson multitaper method. (b) Same as in (a) but for the vertical component of the rotational motion. (c) Dashed line: Half of the ratio between the spectrum in the top panel and the spectrum in the middle panel. Grey line: Theoretical local dispersion of fundamental Love waves as predicted by the local model underneath LCO given by CRUST2.0 combined with the mantle model S20RTS. Solid line: Fundamental Love wave dispersion curve predicted by PREM.

Figure 7. Same as Fig. **??**, but for station LSA.

Figure 8. Same as Fig. **??**, but for station GUMO.

Figure 9. Same as Fig. **??**, but for station WET.

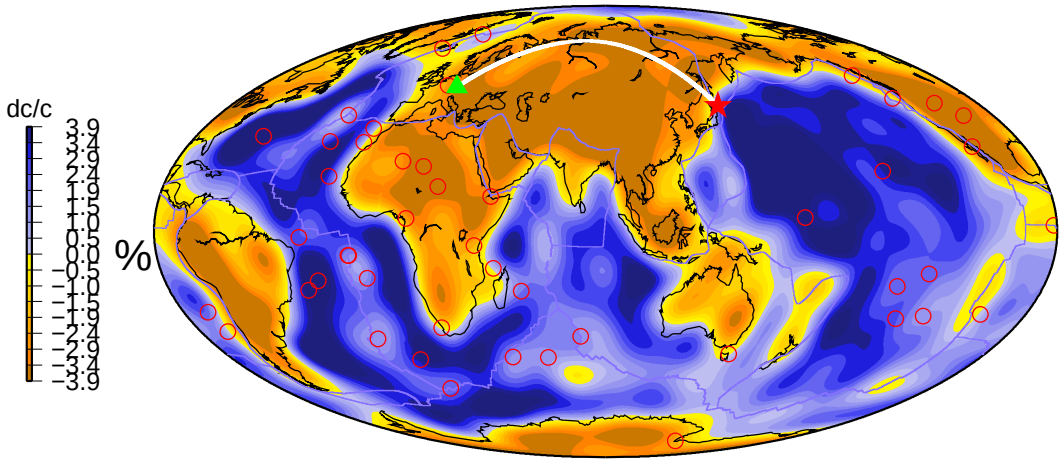

Figure 1: Great-circle path (white line) between the epicenter of the M8.1 September 25 2003 Tokachi-oki earthquake, Japan (red star) and seismic station WET (Lat = 49.15^o, Lon = 12.88^o) near Wettzell, Germany (green triangle), at an epicentral distance of 80^o. These are superimposed on a T=40s fundamental Love wave phase velocity map calculated from the crust model CRUST2.0 combined with the mantle model S20RTS.

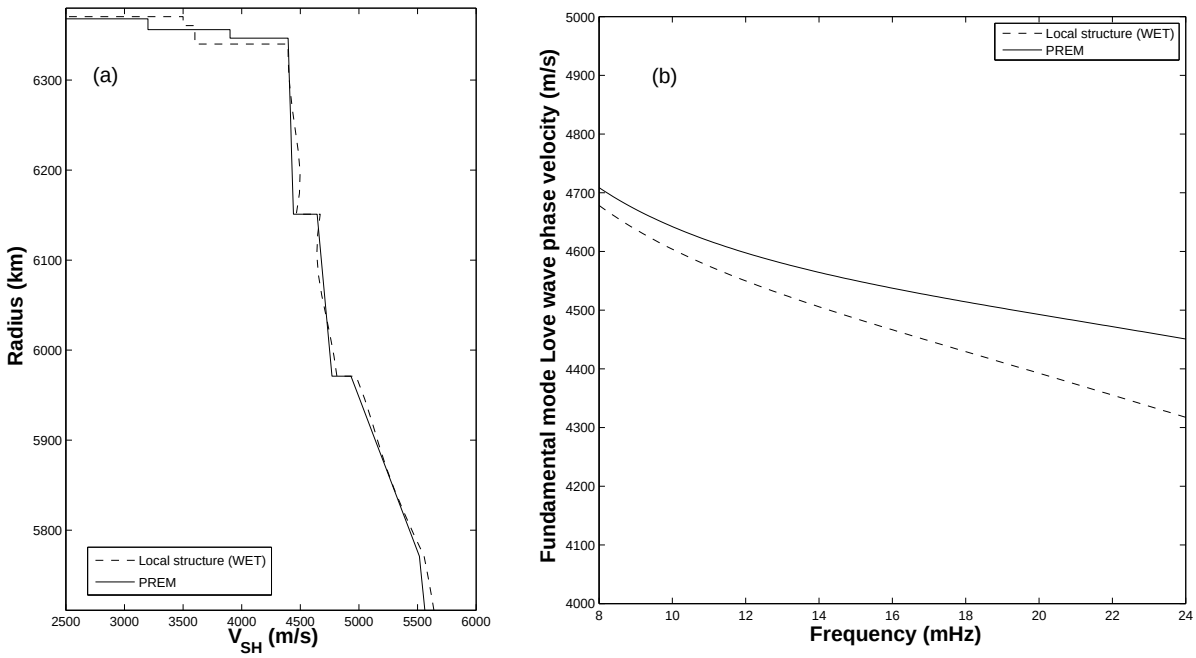

Figure 2: (a)Comparison between PREM shear-wave velocity model (solid line) and the local model beneath the seismic station WET predicted by the crustal model CRUST2.0 combined with the mantle model S20RTS (dashed line). (b) Theoretical local dispersion of fundamental Love waves as predicted by PREM (solid line) and by the local model beneath WET (dashed line).

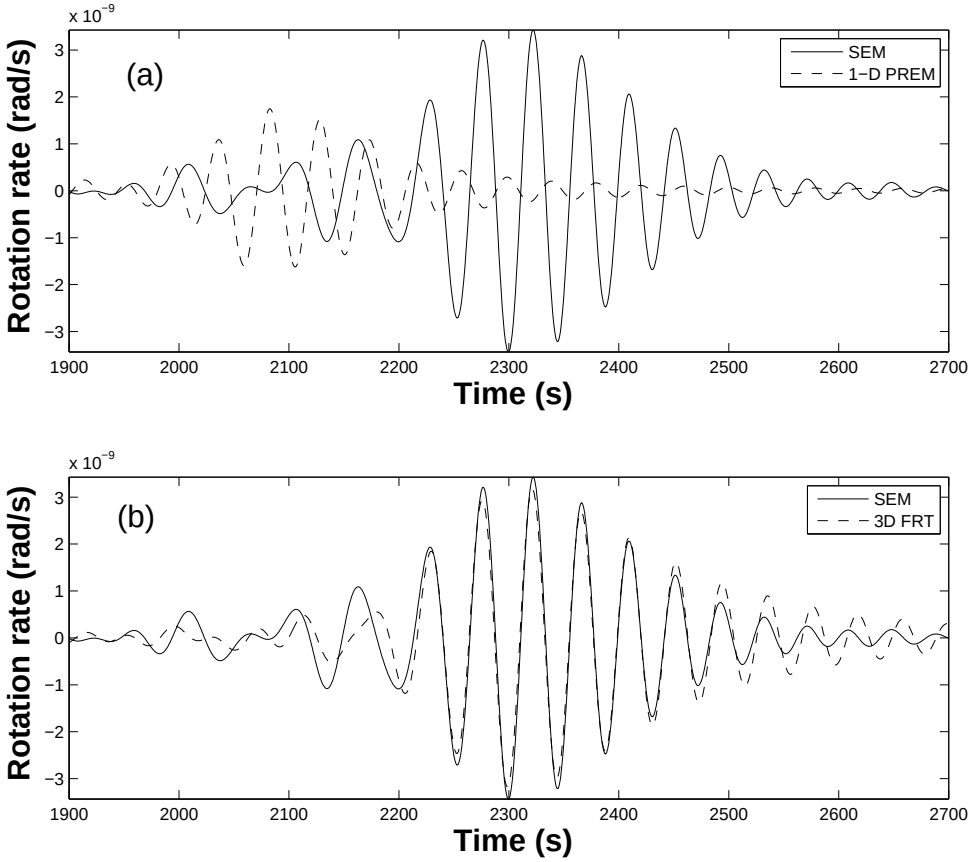

Figure 3: (a) Comparison between spectral-element method (SEM) rotation rate synthetics around a vertical axis using the crustal model CRUST2.0 combined with the mantle model S20RTS (solid line) and mode-summation PREM rotation rate synthetics (dashed line) following the M8.1 September 25 2003 Tokachi-oki earthquake. (b) Comparison between SEM rotation synthetics using the crustal model CRUST2.0 and the mantle model S20RTS (solid line) and full ray theory (FRT) rotation rate synthetics using the same Earth model (dashed line). All the traces have been bandpass filtered around T=40s.

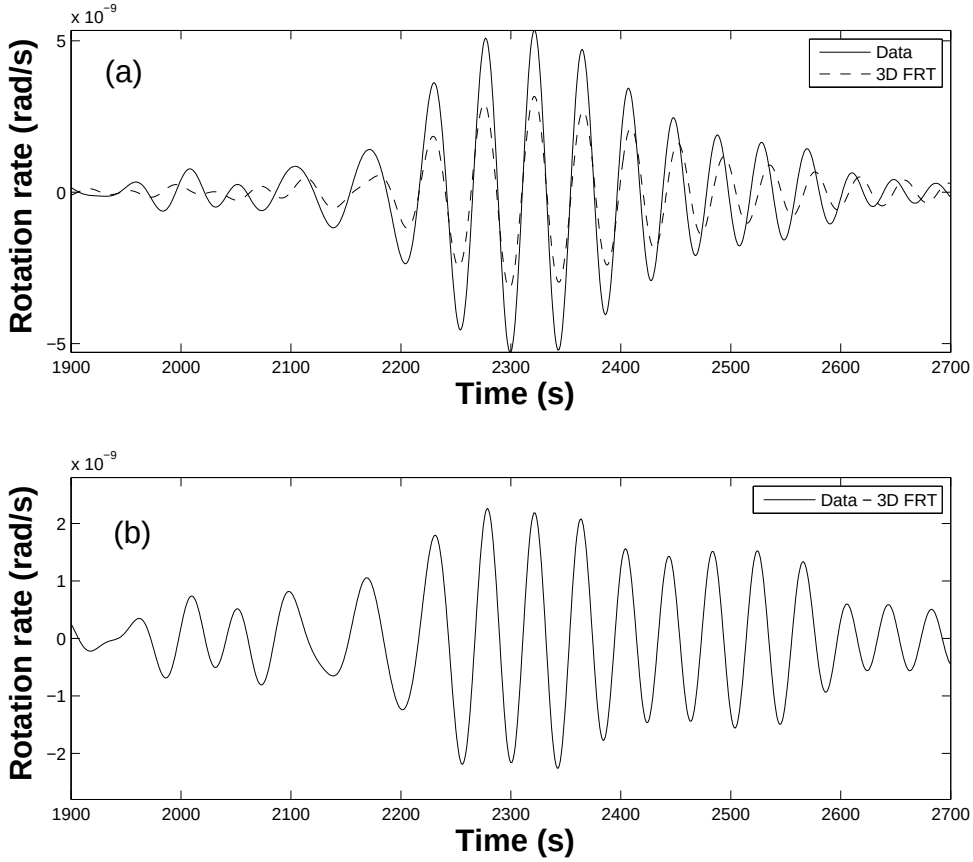

Figure 4: (a) Comparison between observed rotation rate motions around a vertical axis at station WET (solid line) and full ray theory rotation rate synthetics calculated using the crust model CRUST2.0 combined with the mantle model S20RTS (dashed line) for the M8.1 September 25 2003 Tokachi-oki earthquake. (b) Difference between the two traces in the top diagram. All the traces have been bandpass filtered around T=40s.

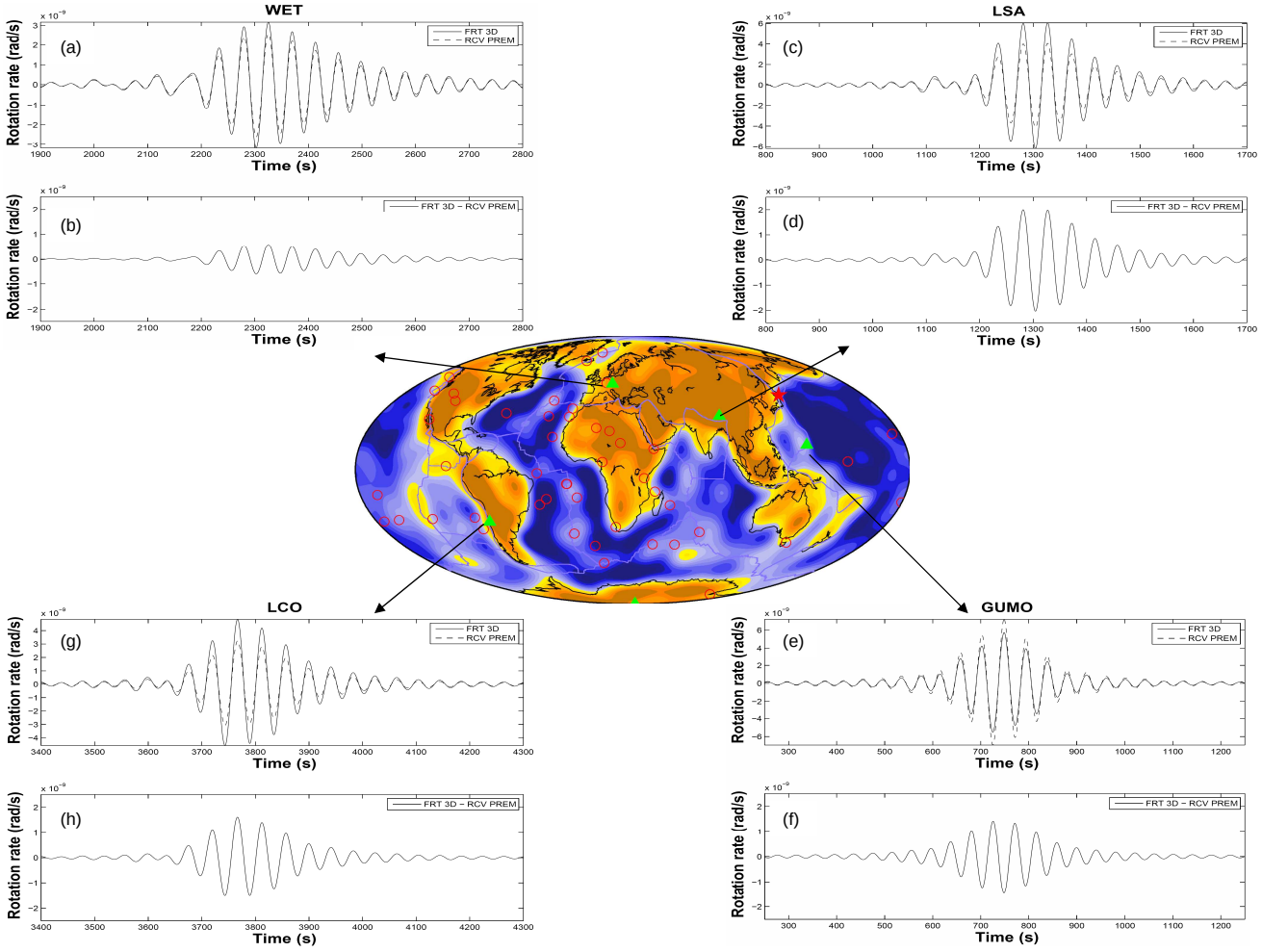

Figure 5: Influence of local structure beneath the receiver for stations within different tectonic environments (green triangles): WET (Germany), LSA (Tibet), GUMO (Marianas Islands) and LCO (Chile). Seismograms are calculated for the M8.1 September 25 2003 Tokachi-oki earthquake (red star). The top diagrams (a,c,e,g) compare rotation rate full ray theory synthetics using the 3-D Earth model (solid line) with " Receiver PREM" synthetics, i.e., calculations using the 3-D Earth model to calculate the source and path terms in the full ray theory Equation 2.7 and using PREM to calculate the receiver term (dashed line); see section 3.2 for details. The traces in the bottom diagrams (b,d,f,h) show the differences between the two seismograms in the top. These differences are due only to deviations of the local shear-wave velocity structure beneath the receiver from PREM.